



Non-perturbative formulation of resonances in quantum mechanics based on exact WKB method

Okuto Morikawa ^{†1} and Shoya Ogawa ^{‡2}

¹*Interdisciplinary Theoretical and Mathematical Sciences Program
(iTHEMS), RIKEN, Wako 351-0198, Japan*

²*Department of Physics, Kyushu University, 744 Motoooka, Nishi-ku,
Fukuoka 819-0395, Japan*

.....
 We study quasi-stationary states in quantum mechanics using the exact WKB analysis as a non-perturbative framework. While previous works focus mainly on stable systems, we explore quasi-stable states such as resonances. As a concrete example, we analyze the inverted Rosen–Morse potential, which exhibits barrier resonance. This model allows exact solutions, enabling a direct comparison with exact WKB predictions. We provide a simple analytic picture of resonance and demonstrate consistency between exact and WKB-based results, extending the applicability of exact WKB analysis to non-polynomial potentials.

[†] okuto.morikawa@riken.jp

[‡] ogawa.shoya.615@m.kyushu-u.ac.jp

1 Introduction

The non-perturbative analysis of quasi-stationary states in quantum mechanics (QM) has long been recognized as an important problem. Recent developments in resurgence theory, particularly in the exact WKB analysis [1–3], have made it possible to formulate these states in a mathematically rigorous and physically meaningful way. Exact WKB analysis has been successfully applied to a wide range of differential equations arising in physical systems: thermodynamic Bethe ansatz equation [4–8], Painlevé equation [9–14], supersymmetry (e.g., Seiberg–Witten curve) [15–25], and cosmology [26–30]. (See also Refs. [31–33].) Also, recently exact WKB analysis—serving as a *non-perturbative formulation of QM*—has been applied to various systems, such as double-well potential [34], periodic-well potential [35], supersymmetric QM [36], and PT -symmetric QM [37, 38]. These developments naturally raise the question: to what extent can such non-perturbative methods deepen our understanding of quasi-stable quantum systems?

Previous research focuses on an eventually stable system while there exist many unstable systems of interest that are quasi-stationary but not stable after decay. A good example is a resonant state. Resonance appears quite universally across various quantum many-body systems: scattering theory, nuclear physics, open quantum systems, and non-Hermitian QM. Such a quasi-stable state is not normalizable. To describe it, we often use analytic continuation or regularization such as the complex scaling method and so on. However, many aspects remain inexplicable because the probability becomes a complex number [39] and a transition cross-section to a resonant state is quite subtle [40, 41]. The complex scaling method [42] seems to work well but is formulated by sophisticated mathematical techniques [43, 44]. Also, it is not transparent how to relate to other methods such as Zel’dovich regularization [45, 46] and rigged Hilbert space [47–49].

In this paper, we investigate quasi-stationary quantum systems based on the exact WKB analysis as a non-perturbative framework. In particular, we aim to understand resonance in this context. As an example, we focus on the inverted Rosen–Morse potential [49, 50]. This system gives rise to the so-called barrier resonance [51] which is not intuitively clear why this is happening. We will give a simple picture from the analyticity. This model is also exactly solvable; we calculate the exact solution of resonant states¹ and compare the consistency of complex energies of resonance with predictions from the exact WKB analysis. Notably, this provides a novel application of the method to a non-polynomial potential.

¹In supersymmetric QM, the system with the (non-inverted) Rosen–Morse potential is a supersymmetric partner of the harmonic oscillator. Then, this allows the derivation of exact solutions; when the inverted case, the corresponding solution is given by the analytic continuation of this explicit expression.

This paper is organized as follows: We first review resonance itself in Sect. 2. At first sight, this is given as pole singularities of an S-matrix. Then some techniques will be introduced to use later. Section 3 introduces the exact WKB analysis. We also consider the cubic potential as a toy model; to derive the quantization condition and understand some kind of decay is required. In Sect. 4.1, we give a simple and general explanation of resonance (including barrier resonance) from the analyticity based on the exact WKB perspective. In Sect. 4.2, we consider the inverted Rosen–Morse potential from the traditional approach and the exact WKB method. We will see the consistency of those complex energies. Section 5 is devoted to the conclusion.

2 Resonant states in scattering theory

Figure 1a shows that bound and resonant states appear as poles of an S-matrix and are characterized by the complex wave number [52]. Resonances exist in the fourth quadrant of the complex k -plane. Bound states are distributed along the negative region of the real axis in the complex E -plane, while resonant states are in the fourth quadrant as shown in Fig. 1b. Note that bound and resonant states exist in the first and second Riemann

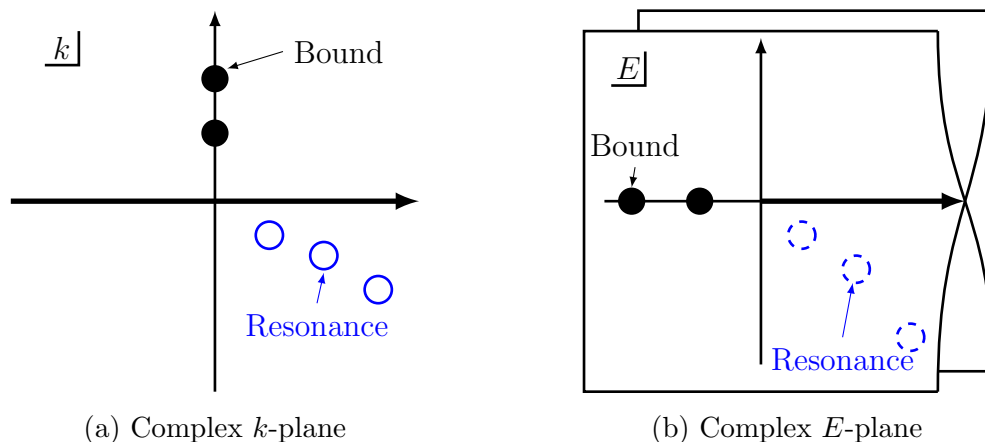


Fig. 1: Distribution of S-matrix poles in (a) the complex k -plane and (b) the complex E -plane. In the right panel (b), the bound states exist in the first Riemann surface, while the resonant states appear in the second Riemann surface.

surfaces, respectively, of the complex E -plane. A resonant state has complex energy, where the real part is the resonant energy and the imaginary part is the decay width. Resonance is produced by the scattering of multiple particles. If the decay width is narrow, a resonant state is observed as a sharp peak in the energy spectrum of the cross-section.

The singular nature of a resonant state, which is the divergence of the wave function in the asymptotic region, causes difficulty in investigating the state. In the 3-dimensional space, the radial wave function $\varphi(r)$ of a resonant state with $k = k_r - ik_i$ ($k_r, k_i \in \mathbb{R}^+$) has the following asymptotic form:

$$\varphi(r) \xrightarrow{r \rightarrow \infty} e^{ikr} = e^{ik_r r} e^{k_i r}, \quad (2.1)$$

which diverges due to the term $e^{k_i r}$. This property also leads to the divergence of the norm, $\|\varphi(r)\|^2$. To obtain a finite value of the norm, the Zel'dovich regularization [45] is introduced as

$$\|\varphi(r)\|^2 \equiv \lim_{\varepsilon \rightarrow +0} \int_0^\infty dr e^{-\varepsilon r^2} \varphi(r)^2 r^2. \quad (2.2)$$

Using this regularization, the orthogonality and completeness properties of the resonant states have been proved by Berggren [46]. It should be noted that the square of the wave function is integrated with the norm of the resonant state.

Recently, the complex scaling method (CSM) [42–44] has been developed as another way to overcome the divergence of the norm and has been applied to describe resonant states of the many-body system, such as nuclei, atoms, and molecules. In the CSM, the coordinate r is transformed as $r \rightarrow e^{i\theta} r$ with a parameter θ . The ABC theorem argues that resonance, which is obtained from a Hamiltonian with this transformation, is square integrable. This can be naively understood as follows: in the CSM, the asymptotic form of the resonant wave function is transformed as

$$e^{ikr} \rightarrow e^{i(k_r - ik_i)re^{i\theta}} = e^{(-k_r \sin \theta + k_i \cos \theta)r} e^{i(k_r \cos \theta + k_i \sin \theta)r}, \quad (2.3)$$

which converges when $\theta > \tan^{-1}(k_i/k_r)$. The CSM thus enables a square-integrable treatment of resonant states by rotating the coordinate into the complex plane and has been successfully applied to many-body systems. Complementary approaches, such as the Gamov shell model [53], have also been developed to tackle the divergence problem inherent in resonant states.

3 Exact WKB analysis and decay rate

3.1 Brief introduction of exact WKB analysis

The 1-dimensional Schrödinger equation can be written as

$$\left[-\frac{\hbar^2}{2} \frac{d^2}{dx^2} + V(x) \right] \psi(x) = E\psi(x). \quad (3.1)$$

For simplicity, we set

$$\left[-\frac{d^2}{dx^2} + \hbar^{-2}Q(x) \right] \psi(x) = 0, \quad Q(x) = 2[V(x) - E]. \quad (3.2)$$

The WKB solution is an ansatz defined by a formal power series,

$$\psi(x, \hbar) = e^{\int^x dx' S(x', \hbar)}, \quad S(x, \hbar) = \sum_{i=-1}^{\infty} \hbar^i S_i(x). \quad (3.3)$$

Substituting $S(x, \hbar)$ into the Schrödinger equation, we have the non-linear Riccati equation; we can obtain the recursive equation of S_i . The leading order of the recursive equation is given by

$$S_{-1}(x) = S_{-1}^{\pm}(x) \equiv \pm \sqrt{Q(x)}. \quad (3.4)$$

It is known that (i) $S_i^- = (-1)^i S_i^+$, (ii) $S^{\pm} = \pm S_{\text{odd}} + S_{\text{even}}$, where $S_{\text{odd}} = \sum_{i=-1,1,3,\dots} \hbar^i S_i^+$ and $S_{\text{even}} = \sum_{i=0,2,4,\dots} \hbar^i S_i$, (iii) $S_{\text{even}} = -\frac{1}{2} \frac{\partial}{\partial x} \ln S_{\text{odd}}$, and also (iv) the exact solution and approximation of the WKB wave function are

$$\psi(x, \hbar)^{\pm} = \frac{1}{\sqrt{S_{\text{odd}}}} e^{\pm \int_{x_0}^x dx' S_{\text{odd}}} \sim \frac{1}{Q^{1/4}} e^{\pm \hbar^{-1} \int_{x_0}^x dx' \sqrt{Q}} + \dots \quad (3.5)$$

The formal series is not necessarily convergent, and one uses the so-called Borel resummation to give a finite value. The essential point is the insertion of one,

$$1 = \frac{1}{\Gamma(n - \alpha)} \int_0^{\infty} dx e^{-x} x^{n+\alpha-1}, \quad (3.6)$$

and exchange of the infinite sum and the above integral. Now, the infinite sum becomes a convergent series, while the integral may be singular for some parameters, called Borel singularity. Then, because the total value is ill-defined, we pick up some analytically continued paths that have an imaginary and non-perturbative nontrivial difference. When the path jumps over the Borel singularity, such a function suddenly changes (Stokes phenomenon). In the exact WKB analysis, we can see such a condition in terms of Q as

$$\text{Im} \hbar^{-1} \int^x dx' \sqrt{Q} = 0. \quad (3.7)$$

The curves determined by this condition are called Stokes curves, and the structure is Stokes graph.

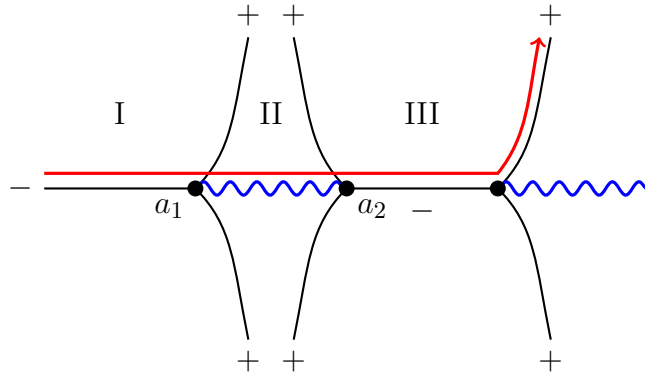


Fig. 2: Stokes graphs for the cubic potential. The black solid curves are the Stokes curves and black points are the turning points connecting three Stokes curves. Blue wavy lines are branch cuts. The red arrowed curve is a possible physical path on which the wave function is defined.

3.2 Application to unstable QM: Anharmonic oscillator with cubic potential

As an example, let us consider the cubic potential, $V(x) = x^2(1 - x)$. This is not well-defined but pedagogical for our purpose. The Stokes graph for $0 < E < \max V(x > 0)$ is shown in Fig. 2. The black solid curves are the Stokes curves. The index of each curve \pm implies that ψ^\pm increases exponentially and

$$\operatorname{Re} \hbar^{-1} \int^x dx' \sqrt{Q} \geq 0. \quad (3.8)$$

Three Stokes curves gather at one point, called the turning point depicted as a black point. Blue wavy lines are branch cuts.

Due to the unbounded potential, it is difficult to define physical phenomena only on $x \in (-\infty, \infty)$. For example, let us choose the red arrowed path and then see what happens. At first, near $x = -\infty$, ψ^- sufficiently decreases and so normalizable. When we jump over the Stokes curve with the index $+$ starting from the same turning point (I \rightarrow II), the Stokes phenomenon gives rise to

$$\begin{pmatrix} \psi_I^+ \\ \psi_I^- \end{pmatrix} = M \begin{pmatrix} \psi_I^+ \\ \psi_I^- \end{pmatrix}, \quad (3.9)$$

where M depends on the rotation of the path around the turning point,

$$M = \begin{cases} M_+ & \text{if anti-clockwise for the index } +, \\ M_+^{-1} & \text{if clockwise for the index } +, \\ M_- & \text{if anti-clockwise for the index } -, \\ M_-^{-1} & \text{if clockwise for the index } -, \end{cases} \quad (3.10)$$

and

$$M_+ = \begin{pmatrix} 1 & i \\ 0 & 1 \end{pmatrix}, \quad M_- = \begin{pmatrix} 1 & 0 \\ i & 1 \end{pmatrix}. \quad (3.11)$$

The above matrix is called the monodromy matrix. Inside region II, we need to connect the different turning points, a_1 and a_2 . The wave function is related to each other by the factor,

$$e^{\pm \int_{a_1}^{a_2} dx S_{\text{odd}}} \quad (3.12)$$

Finally, in the exchange of regions II and III, we again use the connection rule (3.9).

If this system is just the harmonic oscillator, $V(x) = x^2$, the above strategy completes our task. For the wave function to converge near $x = \infty$, we have the quantization condition

$$1 + A = 0, \quad A = e^{\oint dx S_{\text{odd}}}. \quad (3.13)$$

Here the cycle, A , comes from the connection between the turning points a_1 and a_2 . Actually, by analytically continuing, A can be rewritten as the integral around the point of infinity. That is, $A = e^{2\pi i \hbar^{-1} E}$; we have the usual quantized energy spectrum $E = \hbar \left(n + \frac{1}{2} \right)$ with $n \in \mathbb{Z}_{\geq 0}$.

Now, for the cubic potential, the analytical continuation should be stuck because of the branch cut attached to the point of infinity. However, a path on the upper-half plane must differ from that on the lower-half plane. This reproduces the usual result of some kind of tunneling analysis. This section is now finished but we will see a concrete result being identical to the exact solution.

4 Resonant states in exact WKB analysis

4.1 What is a resonant state from the viewpoint of exact WKB?

Given a potential $V(x)$ as a function of $x \in \mathbb{R}$, let us complexify the coordinate as $z \in \mathbb{C}$. In the complex plane z , if the potential $\text{Re } V(z)$ possesses local minima, all of which are not stable physical states, then the Hilbert space of the system includes resonant states. This is

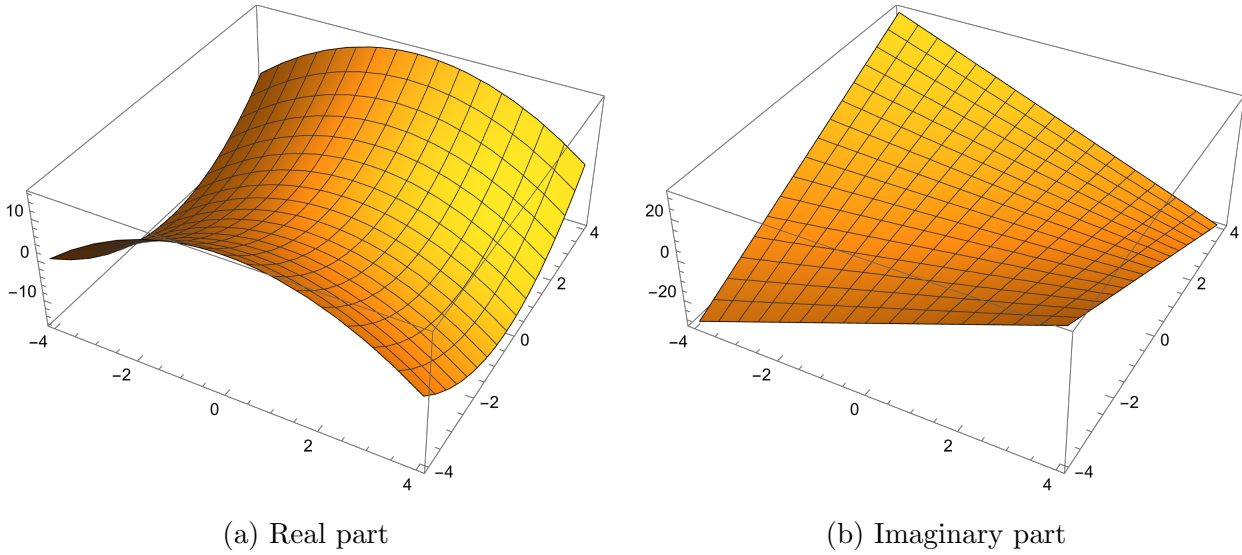


Fig. 3: Potential structure of harmonic oscillator, $-z^2$, in complex plane

because observations from the exact WKB analysis, that is, structures of Stokes curves, are sensitive to the change of signs of $V(z) - E$. For instance, in an unusual harmonic oscillator, $V(x) = -x^2$, one finds that in Fig. 3 there is no local minimum; no resonant state exists. On the other hand, some kind of potential has the local minimum which is not a true vacuum, such as in $1/\cosh^2(x-a) + 1/\cosh^2(x+a)$; there are resonant states. Additionally, it is known that for the potential, $V(x) = 1/\cosh^2 x$, we observe nontrivial complex energies of resonance. This is the so-called barrier resonance, which traps the wave function into the bump. In fact, in Fig. 4, we can see the existence of local minima in $\text{Re } V(z)$ with $\text{Im } z \neq 0$.

In what follows, we focus on an exactly solvable model, where we can see barrier resonant states explicitly. Also, from the above picture, we will have the same complex energies by using the exact WKB analysis.

4.2 Inverted Rosen–Morse potential

4.2.1 Exact solution

Let us consider the inverted Rosen–Morse potential defined by

$$\left[-\frac{\hbar^2}{2m} \frac{d^2}{dx^2} + \frac{U_0}{\cosh^2 \beta x} \right] \psi(x) = E\psi(x), \quad U_0 > 0. \quad (4.1)$$

This Schrödinger equation is exactly solvable as follows: By using $\xi = \tanh \beta x$ and

$$k = \frac{\sqrt{2mE}}{\hbar}, \quad -\frac{2mU_0}{\beta^2 \hbar^2} = s(s+1), \quad s = \frac{1}{2} \left(-1 + \sqrt{1 - \frac{8mU_0}{\beta^2 \hbar^2}} \right) \quad (4.2)$$

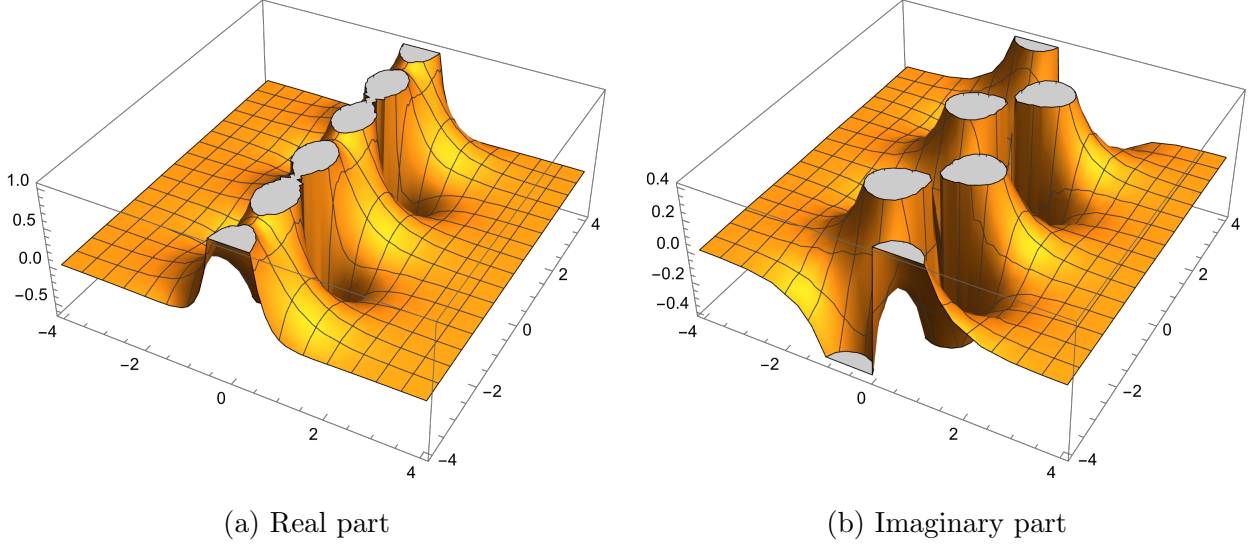


Fig. 4: Potential structure of $1/\cosh^2 z$ in complex plane

the equation can be rewritten as

$$\frac{d}{d\xi} \left[(1 - \xi^2) \frac{d\psi}{d\xi} \right] + \left[s(s+1) - \left(\frac{ik}{\beta} \right)^2 \frac{1}{1 - \xi^2} \right] \psi = 0. \quad (4.3)$$

This is a general Legendre equation. After changing variables as

$$\psi(x) = (1 - \xi^2)^{\frac{ik}{2\beta}} w(\xi) \quad (4.4)$$

and $\frac{1}{2}(1 - \xi) = u$, one finds the hypergeometric differential equation,

$$u(1-u) \frac{d^2}{du^2} w + \left(\frac{ik}{\beta} + 1 \right) (1-2u) \frac{d}{du} w - \left(\frac{ik}{\beta} - s \right) \left(\frac{ik}{\beta} + s + 1 \right) w = 0. \quad (4.5)$$

It is known that there are two independent solutions to the above equation. One solution is finite at $\xi = 1$, that is, $x = \infty$, while another one is divergent there. The former is given by

$$\psi(x) = (1 - \xi^2)^{-\frac{ik}{2\beta}} F \left(-\frac{ik}{\beta} - s, -\frac{ik}{\beta} + s + 1, -\frac{ik}{\beta} + 1, \frac{1 - \xi}{2} \right), \quad (4.6)$$

where F is the Gaussian hypergeometric function.

4.2.2 Traditional approach to resonance

The exact solution (4.6) has complex energies. To see this from the traditional viewpoint, the asymptotic behavior of the solution is of importance. At first, in the case that $x \rightarrow \infty$,

we see

$$(1 - \xi^2)^{-\frac{ik}{2\beta}} \rightarrow 4^{-\frac{ik}{2\beta}} e^{ikx}, \quad (4.7)$$

and

$$F\left(-\frac{ik}{\beta} - s, -\frac{ik}{\beta} + s + 1, -\frac{ik}{\beta} + 1, \frac{1 - \xi}{2}\right) \rightarrow 1. \quad (4.8)$$

Thus, we have the asymptotic form of the exact solution at $x \rightarrow \infty$

$$\psi(x) \rightarrow 4^{-\frac{ik}{2\beta}} e^{ikx}. \quad (4.9)$$

Here, the above expression means the transmitted wave. Next, if $x \rightarrow -\infty$, the overall factor becomes

$$(1 - \xi^2)^{-\frac{ik}{2\beta}} \rightarrow (-4)^{-\frac{ik}{2\beta}} e^{-ikx}. \quad (4.10)$$

On the other hand, noting that

$$\begin{aligned} & F\left(-\frac{ik}{\beta} - s, -\frac{ik}{\beta} + s + 1, -\frac{ik}{\beta} + 1, \frac{1 - \xi}{2}\right) \\ &= \frac{\Gamma\left(1 - \frac{ik}{\beta}\right) \Gamma\left(\frac{ik}{\beta}\right)}{\Gamma(1 + s)\Gamma(-s)} F\left(-\frac{ik}{\beta} - s, -\frac{ik}{\beta} + s + 1, -\frac{ik}{\beta} + 1, \frac{1 + \xi}{2}\right) \\ & \quad + \frac{\Gamma\left(1 - \frac{ik}{\beta}\right) \Gamma\left(-\frac{ik}{\beta}\right)}{\Gamma\left(-\frac{ik}{\beta} - s\right) \Gamma\left(-\frac{ik}{\beta} + s + 1\right)} \left(\frac{1 + \xi}{2}\right)^{\frac{ik}{\beta}} F\left(1 + s, -s, 1 + \frac{ik}{\beta}, \frac{1 + \xi}{2}\right) \end{aligned} \quad (4.11)$$

the hypergeometric function behaves as

$$\begin{aligned} & F\left(-\frac{ik}{\beta} - s, -\frac{ik}{\beta} + s + 1, -\frac{ik}{\beta} + 1, \frac{1 - \xi}{2}\right) \\ & \rightarrow \frac{\Gamma\left(1 - \frac{ik}{\beta}\right) \Gamma\left(\frac{ik}{\beta}\right)}{\Gamma(1 + s)\Gamma(-s)} + \frac{\Gamma\left(1 - \frac{ik}{\beta}\right) \Gamma\left(-\frac{ik}{\beta}\right)}{\Gamma\left(-\frac{ik}{\beta} - s\right) \Gamma\left(-\frac{ik}{\beta} + s + 1\right)} e^{2ikx}. \end{aligned} \quad (4.12)$$

Therefore we have in the $x \rightarrow -\infty$ region

$$\begin{aligned} \psi(x) & \rightarrow (-4)^{-\frac{ik}{2\beta}} e^{-ikx} \frac{\Gamma\left(1 - \frac{ik}{\beta}\right) \Gamma\left(\frac{ik}{\beta}\right)}{\Gamma(1 + s)\Gamma(-s)} \\ & \quad + (-4)^{-\frac{ik}{2\beta}} e^{ikx} \frac{\Gamma\left(1 - \frac{ik}{\beta}\right) \Gamma\left(-\frac{ik}{\beta}\right)}{\Gamma\left(-\frac{ik}{\beta} - s\right) \Gamma\left(-\frac{ik}{\beta} + s + 1\right)}, \end{aligned} \quad (4.13)$$

where the first term on the right-hand side indicates the reflected wave, and the second term is the incident wave. From the Siegert boundary condition [54], the resonant solution is given

in the case that the incident wave vanishes. Hence, $\Gamma\left(-\frac{ik}{\beta} - s\right)$ or $\Gamma\left(-\frac{ik}{\beta} + s + 1\right)$ should be divergent.

- The case that $\Gamma\left(-\frac{ik}{\beta} + s + 1\right)$ diverges.

The divergence point of the Gamma function is expressed as

$$-\frac{ik}{\beta} + s + 1 = -n, \quad n = 0, 1, 2, \dots \quad (4.14)$$

Solving this equation for k , we can obtain

$$k = \frac{\beta}{2} \left[-i \sqrt{\frac{8mU_0}{\beta^2 \hbar^2} - 1} - i(2n + 1) \right]. \quad (4.15)$$

Here, if the inequality, $1 < 8mU_0/(\beta^2 \hbar^2)$, is satisfied, the complex wave number and the complex energy are given by

$$k_n^{\text{R}} = \frac{\beta}{2} \left[\sqrt{\frac{8mU_0}{\beta^2 \hbar^2} - 1} - i(2n + 1) \right] \quad (4.16)$$

and

$$E_n^{\text{R}} = \frac{\hbar^2 \beta^2}{8m} \left[\sqrt{\frac{8mU_0}{\beta^2 \hbar^2} - 1} - i(2n + 1) \right]^2, \quad (4.17)$$

respectively. The wave number is in the fourth quadrant of the complex k -plane. Therefore, this solution corresponds to a resonant state.

- The case that $\Gamma\left(-\frac{ik}{\beta} - s\right)$ diverges.

In the same way as the above case, we can obtain the divergence point of the Gamma function as

$$-\frac{ik}{\beta} - s = -n \quad n = 0, 1, 2, \dots, \quad (4.18)$$

which gives

$$k_n^{\text{AR}} = \frac{\beta}{2} \left[-\sqrt{\frac{8mU_0}{\beta^2 \hbar^2} - 1} - i(2n + 1) \right] \quad (4.19)$$

and

$$E_n^{\text{AR}} = \frac{\hbar^2 \beta^2}{8m} \left[\sqrt{\frac{8mU_0}{\beta^2 \hbar^2} - 1} + i(2n + 1) \right]^2. \quad (4.20)$$

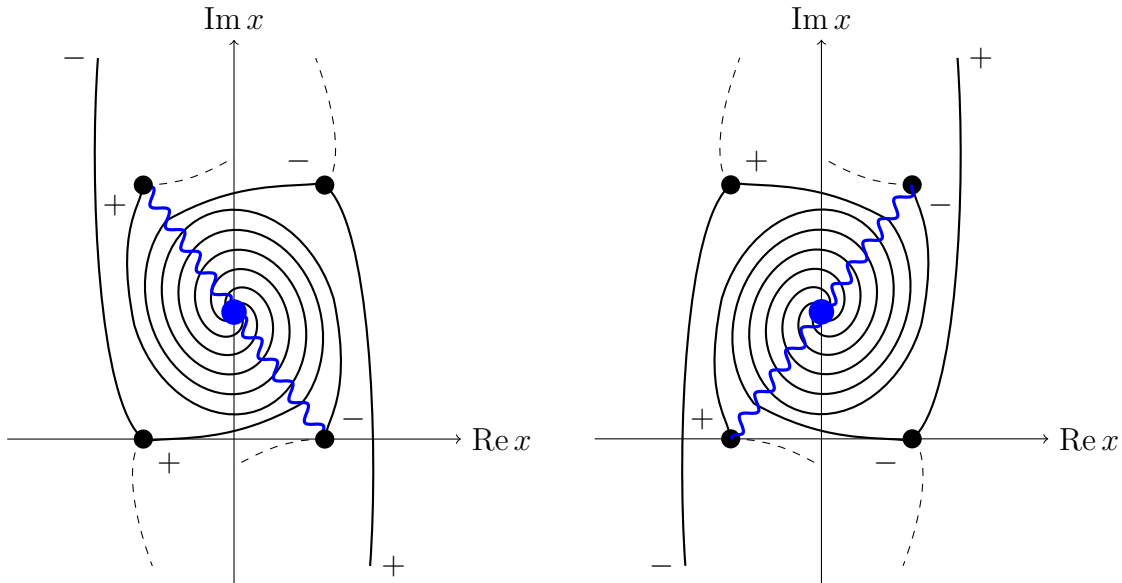


Fig. 5: Schematically illustrated Stokes graph for the inverted Rosen–Morse potential, $V(x) = 1/\cosh^2 x$. The left panel is devoted to $\text{Im } \hbar > 0$ and the right panel is $\text{Im } \hbar < 0$. The black points denote the turning points and the solid curves are the corresponding Stokes curves. The dashed ones, also Stokes curves, mean the periodicity of $\text{Im } x \in [-\pi/2, \pi/2]$ due to the cosine function on $\text{Re } x = 0$. The blue point is the double pole and the blue wavy lines are branch cuts.

The wave number is in the third quadrant of the complex k -plane. Equations (4.16) and (4.19) satisfy the following relation:

$$k_n^{\text{R}} = -(k_n^{\text{AR}})^*, \quad (4.21)$$

which means that the state with k_n^{AR} is a time-reversal state of the resonant state, so-called “anti-resonant state”.

4.2.3 Stokes graph

So far, we have derived the exact resonant solution and its energy. Here, we move with the perspective of the exact WKB analysis. Figure 5 shows the Stokes graph for the inverted Rosen–Morse potential, $V(x) = 1/\cosh^2 x$, with $0 < E < 1$. The left and right panels are devoted to $\text{Im } \hbar > 0$ and $\text{Im } \hbar < 0$, respectively. The black points denote the turning points and the solid/dashed curves are the corresponding Stokes curves. Note that the potential possesses the periodicity of $\text{Im } x \in [-\pi/2, \pi/2]$ due to the cosine function on $\text{Re } x = 0$. The blue point is the double pole and the blue wavy lines are branch cuts.

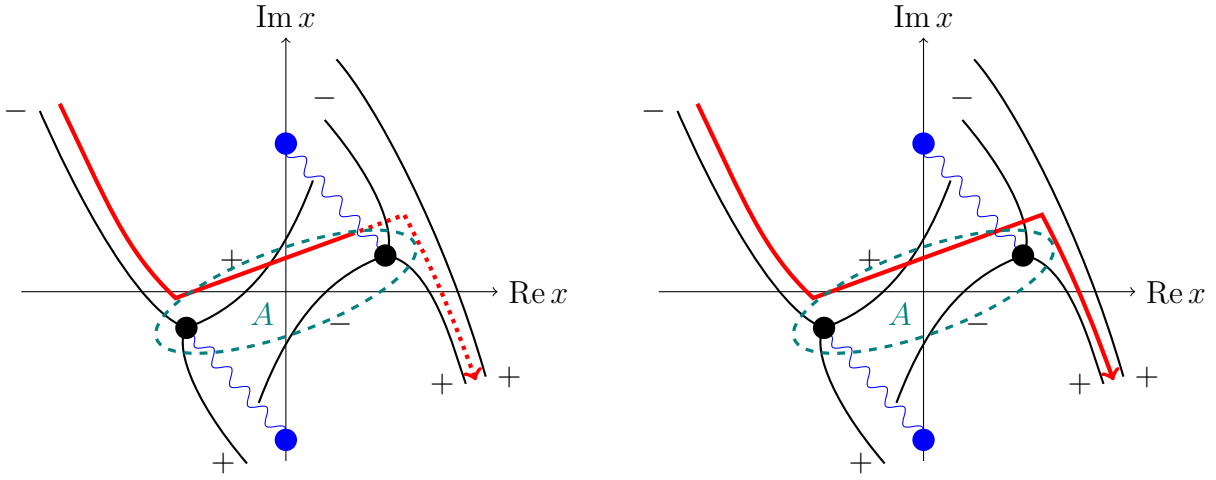


Fig. 6: Quantization condition with $\text{Im } \hbar > 0$ and $\text{Im } E < 0$. The red paths are options to carry out the analytical continuation, along which we can normalize the exact WKB solution on the left panel but cannot have any solution on the right panel. The nontrivial cycle, A -cycle, is shown as the green dashed loop.

To see the resonant states, we choose a path of the analytic continuation from $\text{Im } x \rightarrow \pm\infty$ to $\text{Im } x \rightarrow \mp\infty$ along the Stokes curves depicted in Fig. 5. Especially, because of normalizability, we need to take ψ_- for both regions of $\text{Im } x \rightarrow \pm\infty$. Such a path can be chosen in Fig. 6. The red path on the left panel implies the path in the above sense. On the right panel, the monodromy coefficient should vanish. Note that the red solid curve is on the Riemann sheet depicted while the red dashed curve is on another Riemann sheet after passing through the branch cut.

Figure 6 gives rise to the quantization condition along the red arrowed path on the left panel as

$$1 - A = 0, \quad (4.22)$$

while that on the right panel is

$$1 + A = 0. \quad (4.23)$$

Here, A is the nontrivial cycle, A -cycle, shown as the green dashed loop. From now on, let us calculate A in the leading order of the exact WKB and a completely exact analysis.

4.2.4 Leading order

In the leading order, we carry out an integral of the WKB approximation between the turning points:

$$\int_{-\cosh^{-1}\sqrt{\frac{1}{E}}}^{\cosh^{-1}\sqrt{\frac{1}{E}}} dx \sqrt{2(V(x) - E)} = \sqrt{2} \int dx \sqrt{\frac{1}{\cosh^2 x} - E}. \quad (4.24)$$

Here we set almost all parameters as units for simplicity. After some calculations, we find that

$$\begin{aligned} & \int_{-\cosh^{-1}\sqrt{\frac{1}{E}}}^{\cosh^{-1}\sqrt{\frac{1}{E}}} dx \sqrt{2(V(x) - E)} \\ &= -2 \cosh(x) \sqrt{\frac{-E - \tanh^2(x) + 1}{E \cosh(2x) + E - 2}} \\ & \quad \times \left[\tanh^{-1} \left(\frac{\sqrt{2} \sinh(x)}{\sqrt{E \cosh(2x) + E - 2}} \right) - \sqrt{E} \sinh^{-1} \left(\frac{\sinh(x)}{\sqrt{1 - \frac{1}{E}}} \right) \right] \end{aligned} \quad (4.25)$$

$$= \mp \sqrt{2} i \left[\tanh^{-1} \left(\frac{\sqrt{2} \sinh(x)}{\sqrt{E \cosh(2x) + E - 2}} \right) - \sqrt{E} \sinh^{-1} \left(\frac{\sinh(x)}{\sqrt{1 - \frac{1}{E}}} \right) \right] \quad (4.26)$$

$$= \pm \sqrt{2} \pi (1 + \sqrt{E}). \quad (4.27)$$

Then, from the quantization condition (4.22),

$$2\sqrt{2}\pi(1 + \sqrt{E}) = 2\pi i n, \quad (4.28)$$

with $n \in \mathbb{Z}$. Therefore, the leading complex energy is given by

$$E = \left(1 - \frac{in}{\sqrt{2}} \right)^2. \quad (4.29)$$

This is quite suggestive because we observe resonance even in the leading order of the exact WKB method.

4.2.5 Exact WKB analysis for resonance

In the above Stokes graphs, the exact solution on the normalizable path is explicitly written by the exact solution (4.6). Note that another solution has opposite signs for Stokes

curves. This means that the WKB solution can be exactly given by

$$e^{2 \int_{x_0}^x dx' S_{\text{odd}}} = (1 - \xi^2)^{-\frac{ik}{2\beta}} F \left(-\frac{ik}{\beta} - s, -\frac{ik}{\beta} + s + 1, -\frac{ik}{\beta} + 1, \frac{1 - \xi}{2} \right) \Big|_{\text{at } x}, \quad (4.30)$$

where x_0 is a reference point. The A -cycle, $e^{\oint S_{\text{odd}}}$, between turning points $\mp \cosh^{-1} \sqrt{U_0/E}$ can be realized by the exchange of reference points. That is,

$$e^{2 \int_{x_0}^{\cosh^{-1} \sqrt{U_0/E}} dx S_{\text{odd}}} \times e^{-2 \int_{x_0}^{-\cosh^{-1} \sqrt{U_0/E}} dx S_{\text{odd}}} = e^{2 \int_{-\cosh^{-1} \sqrt{U_0/E}}^{\cosh^{-1} \sqrt{U_0/E}} dx S_{\text{odd}}}. \quad (4.31)$$

Here, we use the formula of the hypergeometric function as

$$\begin{aligned} & F \left(-\frac{ik}{\beta} - s, -\frac{ik}{\beta} + s + 1, -\frac{ik}{\beta} + 1, \frac{1 \pm |\xi|}{2} \right) \\ &= \mathfrak{A} F \left(-\frac{ik}{2\beta} - \frac{s}{2}, -\frac{ik}{2\beta} + \frac{s+1}{2}, \frac{1}{2}, |\xi|^2 \right) \mp \mathfrak{B} F \left(-\frac{ik}{2\beta} - \frac{s-1}{2}, -\frac{ik}{2\beta} + \frac{s}{2} + 1, \frac{3}{2}, |\xi|^2 \right), \end{aligned} \quad (4.32)$$

where

$$\mathfrak{A} = \frac{\Gamma \left(-\frac{ik}{\beta} + 1 \right) \Gamma \left(\frac{1}{2} \right)}{\Gamma \left(-\frac{ik}{2\beta} - \frac{s-1}{2} \right) \Gamma \left(-\frac{ik}{2\beta} + \frac{s}{2} + 1 \right)}, \quad \mathfrak{B} = \frac{\Gamma \left(-\frac{ik}{\beta} + 1 \right) \Gamma \left(-\frac{1}{2} \right)}{\Gamma \left(-\frac{ik}{2\beta} - \frac{s}{2} \right) \Gamma \left(-\frac{ik}{2\beta} + \frac{s+1}{2} \right)}. \quad (4.33)$$

From the fact that $A = 1$ for the existence of a normalizable solution, it is easy to find $\mathfrak{B} = 0$. Therefore $\Gamma \left(-\frac{ik}{2\beta} - \frac{s}{2} \right)$ or $\Gamma \left(-\frac{ik}{2\beta} + \frac{s+1}{2} \right)$ should be at pole singularities. The former corresponds to anti-resonance and the latter is resonance, being identical to the above observation in Sect. 4.2.2 with even numbers of nodes. On the other hand, to vanish non-normalizable solutions, we know $A = -1$; then, $\Gamma \left(-\frac{ik}{2\beta} - \frac{s-1}{2} \right)$ or $\Gamma \left(-\frac{ik}{2\beta} + \frac{s}{2} + 1 \right)$ should diverge such that $\mathfrak{A} = 0$. This is a completely identical result to the complex energies with odd numbers of nodes.

5 Conclusion

In this paper, we have explored quasi-stationary quantum systems through the lens of the exact WKB analysis, focusing on resonant states as a representative example of unstable phenomena. By studying the inverted Rosen–Morse potential—a non-polynomial potential exactly solvable system—we have shown how complex energies can be understood both from direct solution and from exact WKB quantization. This approach provides a clear and analytically consistent picture of resonance, including barrier resonance. We demonstrated the strength of exact WKB methods beyond conventional settings.

Our results suggest that the exact WKB framework offers a promising route to systematically understand non-perturbative aspects of resonance, potentially bridging connections with other methods such as complex scaling and rigged Hilbert space formulations. Further applications to more general systems would be a natural extension of this work.

Acknowledgements

We would like to thank the organizers of Nambu Colloquium at Osaka University. This work was partially supported by Japan Society for the Promotion of Science (JSPS) Grant-in-Aid for Scientific Research Grant Numbers 22KJ2096 (O.M.) and JP21H04975 (S.O.). O.M. acknowledges the RIKEN Special Postdoctoral Researcher Program.

References

- [1] A. Voros, “The return of the quartic oscillator. the complex wkb method,” *Ann. Inst. Henri Poincaré* **39** no. 3, (1983) 211–338.
- [2] E. Delabaere and F. Pham, “Resurgent methods in semi-classical asymptotics,” *Ann. Inst. Henri Poincaré* **71** (1999) 1–94.
- [3] K. Iwaki and T. Nakanishi, “Exact WKB analysis and cluster algebras,” *J. Phys. A* **47** no. 47, (2014) 474009, [arXiv:1401.7094 \[math.CA\]](#).
- [4] K. Ito, M. Mariño, and H. Shu, “TBA equations and resurgent Quantum Mechanics,” *JHEP* **01** (2019) 228, [arXiv:1811.04812 \[hep-th\]](#).
- [5] K. Ito and H. Shu, “TBA equations for the Schrödinger equation with a regular singularity,” *J. Phys. A* **53** no. 33, (2020) 335201, [arXiv:1910.09406 \[hep-th\]](#).
- [6] Y. Emery, “TBA equations and quantization conditions,” *JHEP* **07** (2021) 171, [arXiv:2008.13680 \[hep-th\]](#).
- [7] K. Ito and J. Yang, “Exact WKB Analysis and TBA Equations for the Stark Effect,” *PTEP* **2024** no. 1, (2024) 013A02, [arXiv:2307.03504 \[hep-th\]](#).
- [8] K. Ito and H. Shu, “TBA equations and exact WKB analysis in deformed supersymmetric quantum mechanics,” *JHEP* **03** (2024) 122, [arXiv:2401.03766 \[hep-th\]](#).
- [9] G. Başar and G. V. Dunne, “Resurgence and the Nekrasov-Shatashvili limit: connecting weak and strong coupling in the Mathieu and Lamé systems,” *JHEP* **02** (2015) 160, [arXiv:1501.05671 \[hep-th\]](#).
- [10] K. Iwaki, “2-Parameter τ -Function for the First Painlevé Equation: Topological Recursion and Direct Monodromy Problem via Exact WKB Analysis,” *Commun. Math. Phys.* **377** no. 2, (2020) 1047–1098, [arXiv:1902.06439 \[math-ph\]](#).
- [11] L. Hollands and A. Neitzke, “Exact WKB and abelianization for the T_3 equation,” *Commun. Math. Phys.* **380** no. 1, (2020) 131–186, [arXiv:1906.04271 \[hep-th\]](#).
- [12] K. Imaizumi, “Exact WKB analysis and TBA equations for the Mathieu equation,” *Phys. Lett. B* **806** (2020) 135500, [arXiv:2002.06829 \[hep-th\]](#).
- [13] A. van Spaendonck and M. Vonk, “Painlevé I and exact WKB: Stokes phenomenon for two-parameter transseries,” *J. Phys. A* **55** no. 45, (2022) 454003, [arXiv:2204.09062 \[hep-th\]](#).
- [14] F. Del Monte and P. Longhi, “The threefold way to quantum periods: WKB, TBA equations and q-Painlevé,” *SciPost Phys.* **15** no. 3, (2023) 112, [arXiv:2207.07135 \[hep-th\]](#).
- [15] A.-K. Kashani-Poor and J. Troost, “Pure $\mathcal{N} = 2$ super Yang-Mills and exact WKB,” *JHEP* **08** (2015) 160, [arXiv:1504.08324 \[hep-th\]](#).
- [16] A.-K. Kashani-Poor, “Quantization condition from exact WKB for difference equations,” *JHEP* **06** (2016) 180, [arXiv:1604.01690 \[hep-th\]](#).
- [17] S. K. Ashok, D. P. Jatkar, R. R. John, M. Raman, and J. Troost, “Exact WKB analysis of $\mathcal{N} = 2$ gauge theories,” *JHEP* **07** (2016) 115, [arXiv:1604.05520 \[hep-th\]](#).
- [18] S. K. Ashok, P. N. Bala Subramanian, A. Bawane, D. Jain, D. P. Jatkar, and A. Manna, “Exact WKB Analysis of $\mathbb{C}\mathbb{P}^1$ Holomorphic Blocks,” *JHEP* **10** (2019) 075, [arXiv:1907.05031 \[hep-th\]](#).
- [19] F. Yan, “Exact WKB and the quantum Seiberg-Witten curve for 4d $\mathcal{N} = 2$ pure $SU(3)$ Yang-Mills. Abelianization,” *JHEP* **03** (2022) 164, [arXiv:2012.15658 \[hep-th\]](#).

- [20] K. Imaizumi, “Quantum periods and TBA equations for $\mathcal{N} = 2$ $SU(2)$ $N_f = 2$ SQCD with flavor symmetry,” *Phys. Lett. B* **816** (2021) 136270, [arXiv:2103.02248 \[hep-th\]](#).
- [21] A. Grassi, Q. Hao, and A. Neitzke, “Exact WKB methods in $SU(2)$ $N_f = 1$,” *JHEP* **01** (2022) 046, [arXiv:2105.03777 \[hep-th\]](#).
- [22] M. Bianchi, D. Consoli, A. Grillo, and J. F. Morales, “QNMs of branes, BHs and fuzzballs from quantum SW geometries,” *Phys. Lett. B* **824** (2022) 136837, [arXiv:2105.04245 \[hep-th\]](#).
- [23] M. Alim, L. Hollands, and I. Tulli, “Quantum Curves, Resurgence and Exact WKB,” *SIGMA* **19** (2023) 009, [arXiv:2203.08249 \[hep-th\]](#).
- [24] K. Imaizumi, “Quasi-normal modes for the D3-branes and Exact WKB analysis,” *Phys. Lett. B* **834** (2022) 137450, [arXiv:2207.09961 \[hep-th\]](#).
- [25] K. Imaizumi, “Exact conditions for quasi-normal modes of extremal M5-branes and exact WKB analysis,” *Nucl. Phys. B* **992** (2023) 116221, [arXiv:2212.04738 \[hep-th\]](#).
- [26] S. Enomoto and T. Matsuda, “The exact WKB for cosmological particle production,” *JHEP* **03** (2021) 090, [arXiv:2010.14835 \[hep-ph\]](#).
- [27] S. Enomoto and T. Matsuda, “The exact WKB and the Landau-Zener transition for asymmetry in cosmological particle production,” *JHEP* **02** (2022) 131, [arXiv:2104.02312 \[hep-th\]](#).
- [28] S. Enomoto and T. Matsuda, “The Exact WKB analysis and the Stokes phenomena of the Unruh effect and Hawking radiation,” *JHEP* **12** (2022) 037, [arXiv:2203.04501 \[hep-th\]](#).
- [29] S. Enomoto and T. Matsuda, “The Exact WKB analysis for asymmetric scalar preheating,” *JHEP* **01** (2023) 088, [arXiv:2203.04497 \[hep-th\]](#).
- [30] M. Honda, H. Matsui, K. Okabayashi, and T. Terada, “Resurgence in Lorentzian quantum cosmology: no-boundary saddles and resummation of quantum gravity corrections around tunneling saddles,” [arXiv:2402.09981 \[gr-qc\]](#).
- [31] H. Taya, T. Fujimori, T. Misumi, M. Nitta, and N. Sakai, “Exact WKB analysis of the vacuum pair production by time-dependent electric fields,” *JHEP* **03** (2021) 082, [arXiv:2010.16080 \[hep-th\]](#).
- [32] B. Bucciotti, T. Reis, and M. Serone, “An anharmonic alliance: exact WKB meets EPT,” *JHEP* **11** (2023) 124, [arXiv:2309.02505 \[hep-th\]](#).
- [33] T. Suzuki, E. Taniguchi, and K. Iwamura, “Exact WKB analysis for adiabatic discrete-level Hamiltonians,” *Phys. Rev. A* **109** no. 2, (2024) 022225, [arXiv:2311.05871 \[quant-ph\]](#).
- [34] N. Sueishi, S. Kamata, T. Misumi, and M. Ünsal, “On exact-WKB analysis, resurgent structure, and quantization conditions,” *JHEP* **12** (2020) 114, [arXiv:2008.00379 \[hep-th\]](#).
- [35] N. Sueishi, S. Kamata, T. Misumi, and M. Ünsal, “Exact-WKB, complete resurgent structure, and mixed anomaly in quantum mechanics on S^1 ,” *JHEP* **07** (2021) 096, [arXiv:2103.06586 \[quant-ph\]](#).
- [36] S. Kamata, T. Misumi, N. Sueishi, and M. Ünsal, “Exact WKB analysis for SUSY and quantum deformed potentials: Quantum mechanics with Grassmann fields and Wess-Zumino terms,” *Phys. Rev. D* **107** no. 4, (2023) 045019, [arXiv:2111.05922 \[hep-th\]](#).
- [37] S. Kamata, “Exact WKB analysis for PT-symmetric quantum mechanics: Study of the Ai-Bender-Sarkar conjecture,” *Phys. Rev. D* **109** no. 8, (2024) 085023, [arXiv:2401.00574 \[hep-th\]](#).
- [38] S. Kamata, “Exact quantization conditions and full transseries structures for PT symmetric anharmonic oscillators,” *Phys. Rev. D* **110** no. 4, (2024) 045022, [arXiv:2406.01230 \[hep-th\]](#).
- [39] T. Berggren, “Expectation value of an operator in a resonant state,” *Physics Letters B* **373** no. 1, (1996) 1–4.
- [40] T. Berggren, “On the treatment of resonant final states in direct reactions,” *Nuclear Physics A* **169** no. 2, (1971) 353–362.
- [41] T. Berggren, “On the interpretation of complex cross sections for production of resonant final states,” *Physics Letters B* **73** no. 4, (1978) 389–392.
- [42] T. Myo, Y. Kikuchi, H. Masui, and K. Katō, “Recent development of complex scaling method for many-body resonances and continua in light nuclei,” *Prog. Part. Nucl. Phys.* **79** (2014) 1–56, [arXiv:1410.4356 \[nucl-th\]](#).
- [43] J. Aguilar and J. M. Combes, “A class of analytic perturbations for one-body schroedinger hamiltonians,” *Commun. Math. Phys.* **22** (1971) 269–279.
- [44] E. Balslev and J. M. Combes, “Spectral properties of many-body schroedinger operators with dilatation-analytic interactions,” *Commun. Math. Phys.* **22** (1971) 280–294.
- [45] Y. B. Zel’dovich, “On the theory of unstable states,” *Zh. Éksp. Teor. Fiz.* **39** (1961) 776. [Sov. Phys. JETP **12**, 542 (1961)].
- [46] T. Berggren, “On the use of resonant states in eigenfunction expansions of scattering and reaction amplitudes,” *Nucl. Phys. A* **109** (1968) 265–287.
- [47] R. de la Madrid, “The rigged Hilbert space approach to the Gamow states,” *J. Math. Phys.* **53** (2012) 102113.
- [48] I. Antoniou, Y. Melnikov, and E. Yarevsky, “The connection between the rigged hilbert space and the

- complex scaling approaches for resonances. the friedrichs model,” *Chaos, Solitons & Fractals* **12** (2001) 2683–2688. Rigged Hilbert space and complex scaling method.
- [49] M. Zhao, “Dynamical resonances and lifetimes in rigged hilbert spaces,” *Phys. Lett. A* **204** (1995) 319–322.
- [50] L. D. Landau and E. M. Lifshits, *Quantum Mechanics: Non-Relativistic Theory*, vol. v.3 of *Course of Theoretical Physics*. Butterworth-Heinemann, Oxford, 1991.
- [51] V. Ryaboy and N. Moiseyev, “Cumulative reaction probability from siegert eigenvalues: Model studies,” *The Journal of Chemical Physics* **98** no. 12, (06, 1993) 9618–9623, https://pubs.aip.org/aip/jcp/article-pdf/98/12/9618/19327646/9618.1_online.pdf.
- [52] J. R. Taylor, *Scattering Theory: The Quantum Theory of Nonrelativistic Collisions*. John Wiley & Sons, Inc., New York, 1972.
- [53] N. Michel, W. Nazarewicz, M. Płoszajczak, and T. Vertse, “Shell model in the complex energy plane,” *Journal of Physics G: Nuclear and Particle Physics* **36** no. 1, (Oct, 2008) 013101.
- [54] A. J. F. Siegert, “On the derivation of the dispersion formula for nuclear reactions,” *Phys. Rev.* **56** (Oct, 1939) 750–752.